

Article

Not peer-reviewed version

Influence of Long-Term Humid Ageing and Temperature on the Mechanical Properties of Hybrid FRP Composite Specimens

[Getahun Tefera](#)*, [Glen Bright](#), Sarp Adali

Posted Date: 10 July 2024

doi: 10.20944/preprints202407.0738.v1

Keywords: hybrid composite laminate; RTM; mechanical properties; temperature-dependent properties; empirical models



Preprints.org is a free multidiscipline platform providing preprint service that is dedicated to making early versions of research outputs permanently available and citable. Preprints posted at Preprints.org appear in Web of Science, Crossref, Google Scholar, Scilit, Europe PMC.

Copyright: This is an open access article distributed under the Creative Commons Attribution License which permits unrestricted use, distribution, and reproduction in any medium, provided the original work is properly cited.

Article

Influence of Long-Term Humid Ageing and Temperature on the Mechanical Properties of Hybrid FRP Composite Specimens

Getahun Tefera *, Glen Bright and Sarp Adali

Discipline of Mechanical Engineering, University of KwaZulu-Natal, Durban, South Africa;
Brightg@ukzn.ac.za (G.B.); adail@ukzn.ac.za (S.A.)

* Correspondence: Teferag@ukzn.ac.za.

Abstract: Present experimental study assesses the mechanical properties of glass/carbon/glass hybrid composite laminates after exposure to moisture and elevated temperatures for extended periods. The top and bottom layers of the hybrid laminates are glass fiber reinforced and the middle layer is carbon fiber reinforced with the matrix specified as a polymer material. The hybrid laminates were manufactured using the resin transfer molding method and their compressive and tensile properties were determined using a tensile testing machine. The material parameters such as the storage modulus, the loss modulus, and the damping factors of the laminates were identified using dynamic mechanical analysis as a function of the temperature and the vibration frequency. The experimental results on compressive and tensile properties revealed slight variations when the hybrid laminates were kept at low temperatures for extended periods. This might occur due to the increasing molecular cross-linking of the polymer network. As the temperature increased, compressive, tensile, storage modules, loss modulus, and damping factors decreased. This might occur due to the increasing mobility of the binder material. Particularly, the highest stiffness parameters were obtained on -80°C/GCG (Glass/Carbon/Glass) laminates due to the presence of beta transition on the glassy region. The relationships between the glass transitions and the targeted frequencies were characterized. The values of the glass transition shift towards higher temperatures as the frequency increases. This might occur due to a reduction in the gaps between the crosslinking of the epoxy network when the frequency increases. The accuracy of the storage modulus results was compared with the empirical models. The model based on the Arrhenius law provided the closest correlation. Meanwhile, another model was observed that was not accurate enough to predict when gamma and beta relaxations occur under a glassy state.

Keywords: hybrid composite laminate; RTM; mechanical properties; temperature-dependent properties; empirical models

1. Introduction

Recently, carbon and glass fibre-reinforced materials have been used in several engineering fields, including aerospace, automotive, marine and civil engineering applications. A particular area of the application of composites is the wind turbine blades owing to their high strength and stiffness-to-weight ratios as well as their excellent corrosion resistance and lower density compared to traditional materials as noted in several studies [1–4]. Carbon fibre has a lower density as well as stronger and stiffer mechanical properties as compared to glass fibre. As such carbon fiber-reinforced composites are used extensively in racing cars, aerospace applications, and wind turbine blades as structural components to optimize their energy efficiency [5]. Despite their advantages, lower strain at failure, lower damping properties, and the higher cost of carbon fibres make their use in these applications challenging [6]. Reducing the cost and obtaining optimum mechanical properties of composite structures are critical considerations in the composite industry. One approach to achieving

tailored material properties is a hybridization of carbon and glass fibres which has the potential to reduce the cost and improve the mechanical performance of the composite structures as noted in [7–9]. Nonetheless, there are concerns about the durability of composite structures exposed to harsh environmental conditions during their operational lifetime as discussed in [10–12]. As such it becomes important to determine the thermo-mechanical performance of fiber-reinforced polymer (FRP) materials under different environmental conditions before using them in various applications.

Several studies investigated the mechanical performance of FRP materials subject to different environmental conditions. For example, the mechanical performance of FRP materials exposed to high temperatures was examined by Bazli and Abolfazli [13] which involved near and above the resin glass transition temperatures. Low levels of degradation were observed below the glass transition temperature (T_g) of the epoxy matrix. High values of T_g have a detrimental effect on the mechanical performance of FRP composites. The polymer matrix softens and weakens the bonding at the fibre/matrix interface when the temperature exceeds (T_g), resulting in the rapid reduction of strength as noted in [14,15]. Cao et al. [16] conducted an experimental study on the tensile properties of pure carbon/epoxy and hybrid carbon fibre combined with glass and basalt fibre sheets at elevated temperatures. The tensile performance of the pure and hybrid sheets was significantly reduced as the temperature increased. Additionally, the tensile, compressive, flexural moduli and energy absorption properties of carbon fibre-reinforced polymer (CFRP) materials under low and high temperatures were investigated in several studies as noted in [17–23]. The compressive and tensile strengths of CFRP laminates severely deteriorated at high temperatures. Whereas, the flexural and energy absorption properties of CFRP laminates improved at lower temperatures. Similarly, Hawileh et al. [24] studied the tensile and stiffness properties of carbon laminates, glass laminates, and the hybrids of the two fibres exposed to ambient and elevated temperatures. Severe reductions in the mechanical performance of the laminates were observed in the case of single material laminates rather than the hybrid laminates.

Long-term effects of moisture on the mechanical performance of CFRP laminates, glass fibre-reinforced polymer (GFRP), and their hybrids have been investigated in [25–27]. The results confirmed that the performance of the laminates was not significantly affected at low temperatures. This might be due to the presence of closely packed epoxy chain segments and the transition of the polymer material into beta and delta relaxation phases in the glassy state as investigated in [28,29].

Spagnuolo et al. [30] studied the tensile properties of GFRP bars under elevated temperatures to replace ordinary steel reinforcements. It is an effective and economical solution to corrosion problems and durability. Additionally, Mathiev and Brahim [31] conducted an experimental study on the flexural, shear, and tensile strength properties of GFRP bars exposed to lower and elevated temperatures. The experimental results confirmed that the flexural, shear, and tensile strengths of GFRP bars increased when the temperature decreased. A change in the mechanical performance was observed when a high level of moisture absorption causes the volume expansion of GFRP bars which aggravates the initiation of microcracks when it freezes [32]. Moreover, the moisture absorption properties of GFRP laminates and their effect on mechanical performance were examined after being immersed in distilled water at ambient and 90°C temperatures [33]. It was observed that the degree of damage strongly depends on the applied temperature. In particular, the moisture uptake of the laminates impairs the fiber/matrix interface which contributes to lowering the mechanical performance in the matrix-dominated direction.

Most composite structures based on FRP composites are used under various environmental conditions. Their mechanical performance needs to be studied further under different environmental conditions and also to improve their working lifetime. In particular, determining the viscoelastic properties of FRP composites such as the glass transition temperature, damping factors, storage modulus, and loss modulus is important for composites exposed to different environmental conditions as noted in [34]. Carbon and glass fibres are the most often used reinforcements for FRP materials. Thermo-mechanical properties of CFRP, GFRP, and hybrid composite laminates have been studied using the dynamic mechanical analysis (DMA) tool after being exposed to moisture for extended periods and to elevated temperatures in the studies [35–38]. The performance of all groups

of laminates showed an increase in stiffness properties, and different relaxation phases were observed in the glassy region for those that have extended humid ageing. However, as the temperature increased, the storage modulus of the composite laminates decreased as expected. This may have occurred due to the mobility of the epoxy matrix networks.

Researchers have been developing theoretical models to predict the thermo-mechanical properties of FRP composites as a function of temperature. The cost of production and the time spent testing the samples can be reduced by utilizing theoretical models rather than using the DMA tool as noted in [39–44]. In particular, Gibson et al. [45] proposed an empirical model to determine the temperature-dependent properties of FRP composites involving the compressive and tensile strengths and the storage modulus. The values of the parameters were studied at the glass transition regions of the polymer materials. The proposed empirical model shows a close correlation with the experimental results obtained for the storage modulus properties of the glass/polyester laminates. Recently, Bai et al. [46] used the Arrhenius law to model the temperature-dependent storage modulus and the viscosity properties of pultruded glass fibre-reinforced polyester laminates under elevated and high temperatures. Moreover, Feng and Guo [47] developed a theoretical model for temperature-frequency-dependent dynamic mechanical properties of epoxy resin and glass/epoxy composites considering the degree of conversion in the glass transition and the decomposition regions. The Arrhenius law has been the best method to determine the mechanical performance of FRP composite material as a function of different temperatures and frequencies.

In the present study, the impact of humid ageing and temperatures on the thermomechanical properties of hybrid glass/carbon/glass (GCG) composite laminates was evaluated experimentally in order to apply the results to the construction of the spar cap section of wind turbine blades. The tensile and compressive properties of the laminates under lower and higher environmental conditions were characterized. Additionally, the stiffness parameters, such as storage modulus, loss modulus, damping properties, and the glass transition temperatures of all groups of hybrid laminates were determined using the DMA tool. Finally, the accuracy of the storage modulus results in relation to the empirical models was assessed at different test temperatures and frequencies. A better candidate for an empirical model that fitted with the experimental results was obtained, and its accuracy was investigated.

2. Experimental Program

A series of hybrid composite laminates were tested in tension, compression, and bending under different environmental conditions. Before testing, the laminates were kept at low and high temperatures, and their mechanical performance was characterized. Particularly, the tensile and compressive properties of GCG groups of hybrid laminates were determined by using a tensile testing machine. Moreover, the storage moduli, loss moduli, damping factors, and glass transition temperatures of the laminates as a function of temperatures and frequencies were determined using the DMA tool.

2.1. Materials

Unidirectional E-glass fibre, unidirectional T-300 carbon fibre, prime 27 LV epoxy resin, and prime 27 LV hardener were used to prepare the GCG group of hybrid composite laminates. The epoxy matrix for all groups of the hybrid specimens was prepared with a weight mixing ratio of 10:2.6. The mechanical and physical properties of the fibres and epoxy resin are shown in Table 1.

Table 1. The mechanical properties of carbon fiber, glass fiber, and the epoxy resin [48].

Materials	Young's modulus [GPa]	Tensile strength [MPa]	Density [Kg/m ³]	Poisson's ratio
T-300 carbon	230	3530	1760	0.30
E-glass	72.5	2350	2570	0.25
Epoxy resin	3.3	69.9	1020	0.36

Hybrid Composite Laminates and Preparation Procedures

The GCG composite laminates were produced using resin transfer molding (RTM) methods, based on ASTM standards given in [49–51]. Compressive, tensile, and bending tests were performed on the hybrid laminates. A total of four layers of fibres were used to construct the hybrid laminates for the tensile and compressive testing processes. Two layers of carbon fibers were used in the middle layers of the hybrid laminates along with a common epoxy resin. In the case of DMA tests, a total of ten layers of fibres were used. Among the ten layers, four layers of carbon fiber were used in the middle of the hybrid laminates with a common epoxy resin as a binder. All specimens were cured at room temperature for 24 hours before being post-cured at 65°C in the oven for 16 hours. The specimens were cut to the desired dimension using a computer numerical control (CNC) machine with a tolerance of 0.02 mm, then cleaned, and the flash was removed using sandpaper. Five samples were considered for each group of hybrid laminates during the testing process.

The volume fractions of the specimens were determined as 55% using burn-off test methods based on ASTM standards [52]. The hybrid composite laminate preparation process, fibre orientation, and the test methods used in this study are shown in Figure 1.

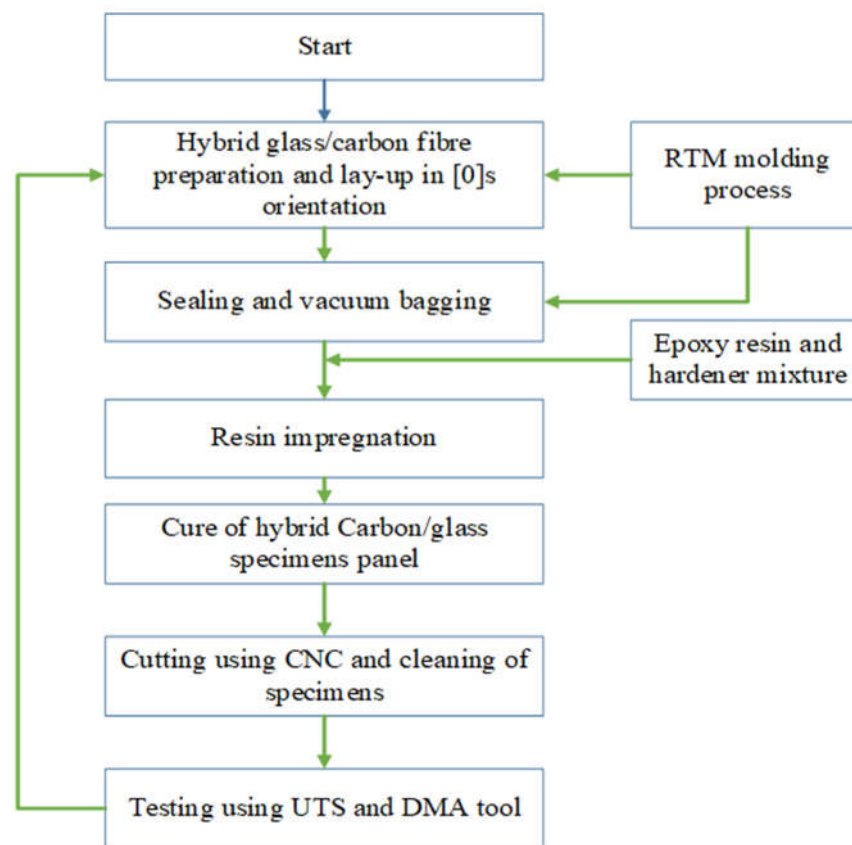


Figure 1. A flow chart for the construction and testing methods of GCG hybrid specimens.

2.2. Test Methods

The compressive and tensile properties of the GCG composite laminates were assessed using a Lloyd LR testing machine by measuring at a rate of 2 mm/min. Before testing, the GCG groups of composite laminates were preserved in a deep freezer at temperatures of -80°C, -20°C, and 0°C for 60 days. Additional specimens were preserved at room temperature, and tests were carried out at lower and higher test temperatures. A heat-con thermocouple was used to measure and control the existing temperatures on each hybrid laminate during the testing process. An Epsilon digital extensometer of 25 mm gauge length was used to determine the strain of hybrid laminates at different testing temperatures.

The dynamic mechanical properties of the GCG composite laminates were measured using a DMA Q 800 TA tool. The hybrid specimens were preserved in a deep freezer at a temperature of -80°C, -20°C, and 0°C for 60 days. Additionally, the controlled GCG specimen was maintained at 25°C before testing. Experimental work was conducted on hybrid specimens under the three-point bending modes using the dynamics oscillation frequency of 1 Hz, 10 Hz and 100 Hz. An amplitude of 15 μm was applied. The heating rate was increased at 2°C/min. Liquid nitrogen was used as the cooling agent. The test temperatures were set for all groups of hybrid laminates ranging from -80°C to 140°C, -20°C to 140°C, 0°C to 140°C, and 20°C to 160°C. The dimensions of the hybrid laminates were set at a height of 4.60 mm, a width of 13 mm and a length of 64 mm to determine the storage modulus (E'), loss modulus (E''), damping factor and glass transition temperature (T_g).

3. Results and Discussion

3.1. Mechanical Properties of the Laminates at Different Ageing Temperatures

3.1.1. Compressive Properties

The compressive properties of GCG groups of composite laminates at different test temperatures are shown in Table 2. Results indicate how the compressive properties of all groups of GCG laminates are dependent on the temperature. The highest and lowest compressive strengths were obtained in the -80°C/GCG and 100°C/GCG groups of composite laminates. The reduction ratios are about 11.78%, 11.49%, 33.94%, 62.66%, 67.54%, and 89.81% as the temperature increases from -80°C to 100°C. This reduction might happen due to the closely compacted nature of polymer molecules at lower temperatures and the ease of mobility under higher environmental conditions. Particularly, as the test temperatures of the laminates were close to T_g of the epoxy matrix, the force needed to break the laminates started to decrease. The reduction in compressive loading and stress distribution as a function of the targeted test temperatures is shown in Figure 2(a). This might occur due to the weak bonding at the fibre/matrix interface. Based on this compressive experimental data, an extended lifetime from the FRP composite structures can be expected when applied to lower environmental conditions.

Table 2. The compressive properties of the hybrid composite laminates at different test temperatures.

Temperature (°C)	Designation of GCG composite laminates	Maximum force during failure (N)	Compressive strength (MPa)	Standard deviation (SD) and coefficient of variation (CV)
-80	-80/GCG	14382.19	668.19	(63.78, 9.54%)
-20	-20/GCG	12072.99	589.46	(60.11, 9.83%)
0	0/GCG	12414.76	591.41	(23.25, 3.93%)
25	25/GCG	9004.27	441.42	(34.34, 7.78%)
50	50/GCG	5572.57	249.47	(21.78, 8.73%)
75	75/GCG	4370.02	216.88	(17.08, 7.87%)
100	100/GCG	1412.86	68.06	(6.39, 9.40%)

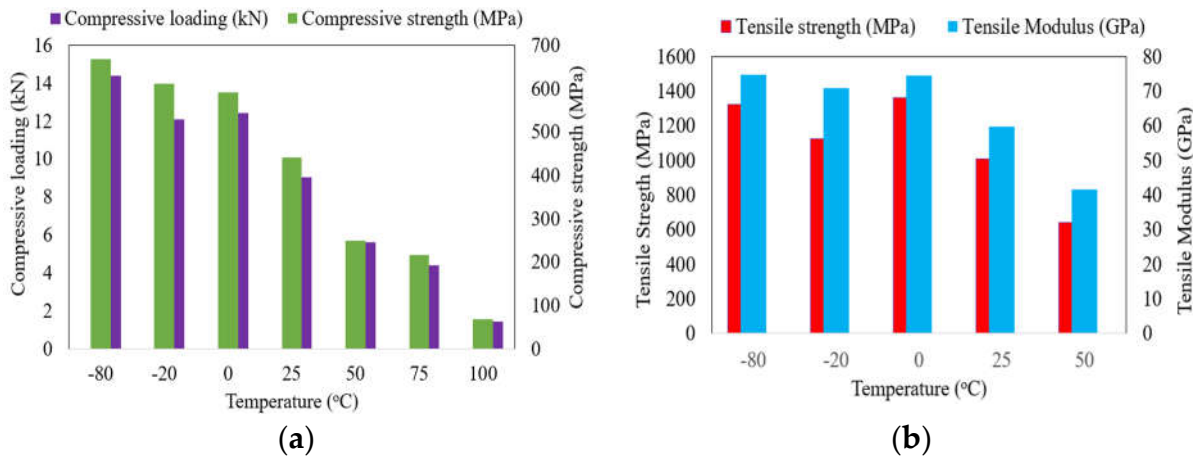


Figure 2. Mechanical properties and failure load of hybrid laminates at various temperatures, (a) compressive properties; and (b) tensile properties.

3.1.2. Tensile and Stiffness Properties

The tensile properties of GCG groups of laminates at various temperatures are listed in Table 3. As the temperature increases to 0°C, 25°C, and 50°C, the tensile strength and tensile modulus of the hybrid laminates decrease. A slight change in the tensile properties was observed as the temperature decreased to -20°C and -80°C. This may occur due to the presence of more moisture which increases the crosslinking network of polymers to optimize the failure limit of the hybrid laminates. Increasing the cross-linking networks improved the bond between fibre/epoxy to delay failure. Compared with the tensile strength of 1358.16 MPa at 0°C, the tensile strengths of GCG groups of laminates were reduced by 25.97% and 53.05% as the temperatures increased to 25°C and 50°C, respectively. Additionally, the tensile modulus of the hybrid laminates changed by 19.60% and 44.16%, respectively. In this case, the mobility of the polymeric molecules increased due to the increase in temperature. Additionally, the bond between the fibre/epoxy was weak, and the load-transferring capacity of the epoxy matrix was reduced, so the forces needed to break the laminates decreased.

Table 3. The tensile properties of the hybrid composite laminates at different test temperatures.

Temperature (°C)	Designation of GCG composite laminates	Force during failure (N)	Tensile strength (MPa), SD, and CV	Tensile modulus (GPa), SD, and (CV)
-80	-80°C/GCG	27234.64	1321.20 (37.53, 2.84%)	74.63 (1.71, 2.29%)
-20	-20°C/GCG	23365.99	1125.01 (35.63, 3.17%)	70.89 (0.53, 0.74%)
0	0°C/GCG	27437.70	1358.16 (29.54, 2.18%)	74.35 (5.64, 7.58%)
25	25°C/GCG	20715.62	1005.39 (92.28, 9.18%)	59.78 (5.14, 8.60%)
50	50°C/GCG	12958.90	637.66 (1.09, 0.17%)	41.55 (3.31, 7.96%)

3.2. Dynamic Mechanical Properties of Hybrid Laminates

DMA tests were conducted to investigate the change in the mechanical properties of four groups of GCG laminates after being preserved at different temperatures. The experimental storage modulus results were normalized by the initial values to minimize small discrepancies at the initial temperatures as shown in Figure 3. It should be noted that the storage modulus of all groups of the laminates decreases when the glass transition occurs and drops further at decomposition. The experimental results confirmed the temperature-dependent mechanical properties of FRP composite materials. Furthermore, the glass transition temperature of the hybrid laminates at the targeted preserved temperatures was characterized. A delay in the T_g value was observed when the hybrid laminates were preserved at lower temperatures for extended periods. This might occur due to the intact bonding properties of polymer molecules at lower temperatures. Particularly, the first

transitions occurred in the case of $-20^{\circ}\text{C}/\text{GCG}$ (-20°C to 17°C) and $-80^{\circ}\text{C}/\text{GCG}$ (-80°C to 17°C) hybrid laminates, this is attributed to the β -relaxation of the polymer chain molecules [28]. The second α -transition is observed in $-20^{\circ}\text{C}/\text{GCG}$ (17°C to 86°C) and $-80^{\circ}\text{C}/\text{GCG}$ (17°C to 90°C) hybrid laminates which corresponds to the glass transitions of the polymer networks. The relationships between the glass transition temperature and the dynamic oscillation frequency are assessed. The results confirmed that the T_g values of the polymer network increased as the frequency increased. This might occur due to a reduction in the gaps between the crosslinking of the polymer network which causes the laminates to behave elastically for extended periods at higher frequencies. Mainly, moisture swelling for extended periods at the lowest temperatures contributed to increasing the storage modulus of the hybrid laminates in the glassy regions. This might occur due to the reduction of the crosslinking of the polymer network which needs a higher temperature to increase the mobility of the polymer molecules.

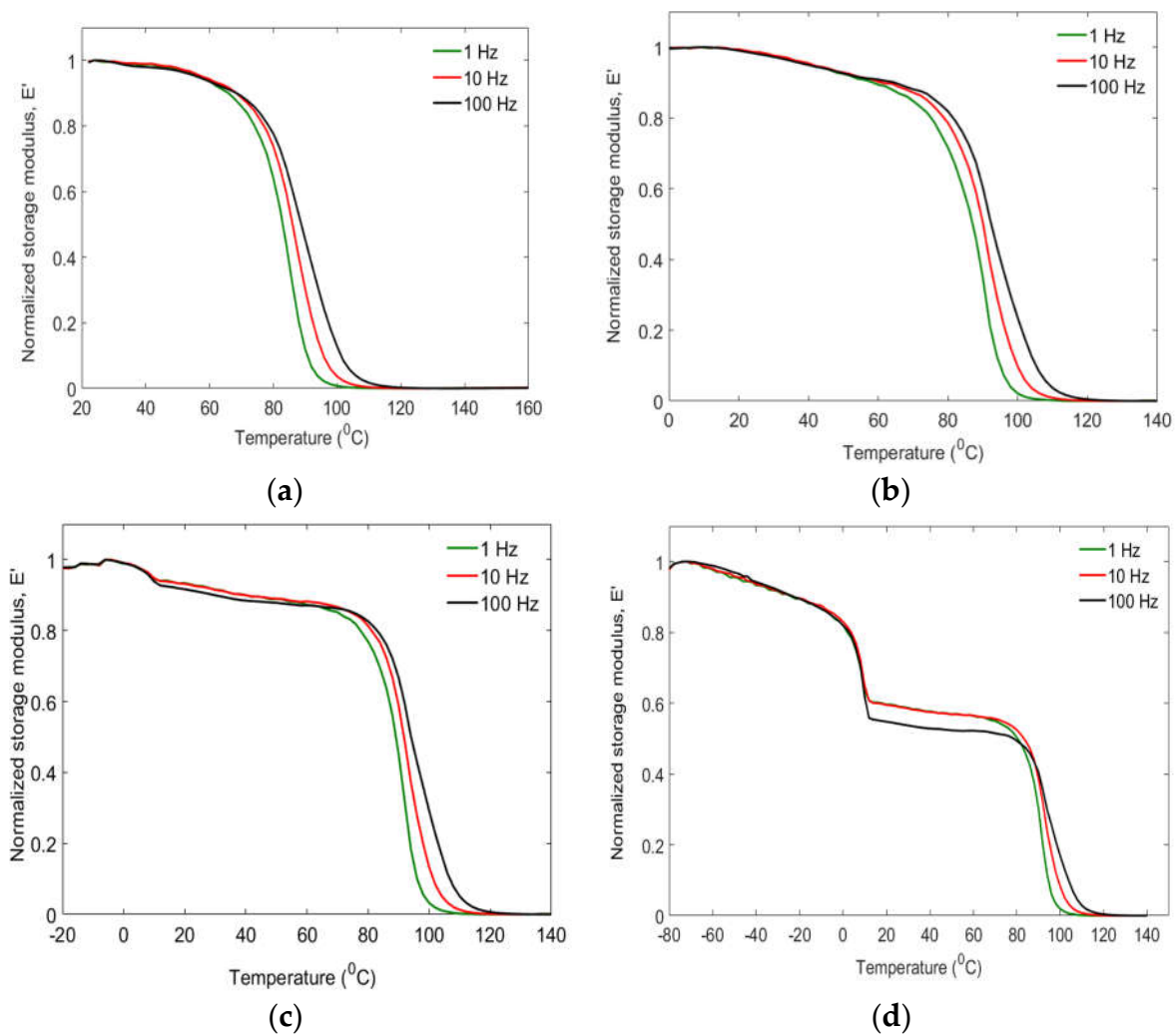


Figure 3. Storage modulus properties of control GCG (a), $0^{\circ}\text{C}/\text{GCG}$ (b), $-20^{\circ}\text{C}/\text{GCG}$ (c), and $-80^{\circ}\text{C}/\text{GCG}$ (d) laminates at various temperatures and frequencies.

The kinetic parameters can be estimated from the experimental materials to be used for developing theoretical models. Mostly, as the temperature is raised, the polymer material changes its state to glassy, leathery, rubbery, and decomposed. The common phase transitions of the polymer material are the glass transition, the leathery to rubbery transition, and the rubbery to decomposition-transition. In the case of $-20^{\circ}\text{C}/\text{GCG}$ and $-80^{\circ}\text{C}/\text{GCG}$ laminates, one additional state, namely beta (β) transition was observed before the glass transition occurred. This happened due to extended periods of swelling of moisture.

It is important to find the kinetic parameters of the hybrid laminates from a glassy to a leathery state to use in developing a theoretical model and applying it to design different composite structural components. The conversion degree at the glass transition region of the four groups of GCG composite laminates can be estimated by the following relation:

$$\alpha_g = \frac{E'_g - E'}{E'_g - E'_r} \quad (1)$$

where E'_g is the storage modulus of the hybrid laminates in the glassy state, E' is the instantaneous storage modulus in the glass transition region, and E'_r is the storage modulus of the hybrid laminates in the rubbery state.

As shown in Figure 4, the conversion degree of the hybrid laminates increased as the testing temperature increased due to the mobility of the polymer molecules. The lowest conversion degree was observed in the case of $-80^\circ\text{C}/\text{GCG}$ laminates. Additionally, the influence of frequencies on the conversion degrees of the hybrid laminates was observed. The values of the conversion degree were lower as the frequency increased. It needs additional time to increase the mobility of the polymer molecules.

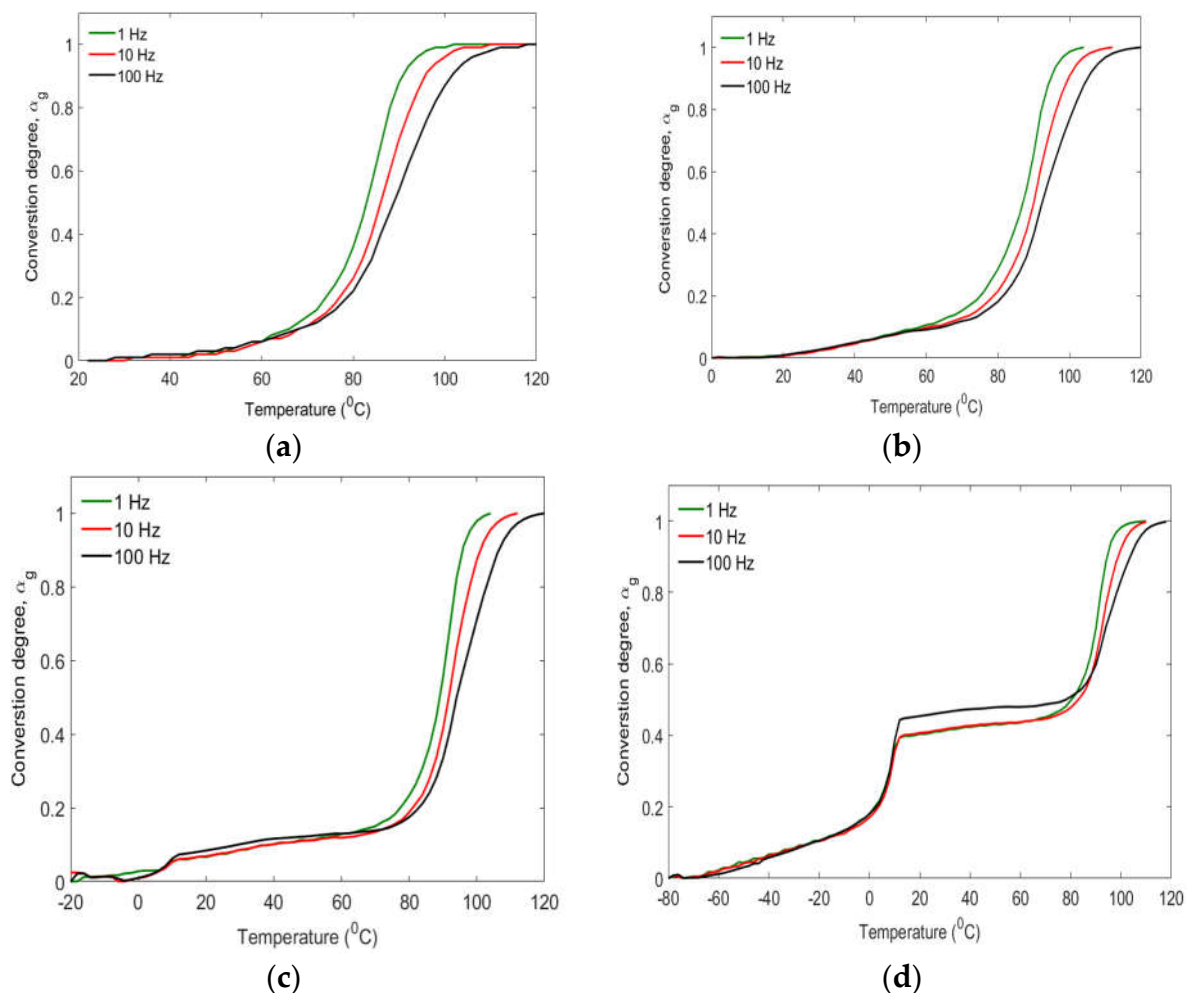


Figure 4. Conversion degree of glass transition (α_g) for modeling the storage modulus of control GCG (a), $-0^\circ\text{C}/\text{GCG}$, $-20^\circ\text{C}/\text{GCG}$, and $-80^\circ\text{C}/\text{GCG}$ hybrid laminates.

The experimental loss modulus and $\tan \delta$ value of four GCG composite laminates under different temperatures and frequencies are characterized in Figure 5. The values of the loss modulus are used to determine the amount of energy dissipated as heat when the FRP composite material turns viscous. The $\tan \delta$ value is the ratio of the loss modulus to the storage modulus properties of the materials which is used to characterize the damping capability of FRP materials. As shown in

Figure 5, the energy dissipation and damping properties of the hybrid laminates reached peaks. This might occur due to the mobilization of the polymer molecules with increasing temperatures. The peaks of the curves are used to determine the glass transition temperature of the material. The values of T_g at the loss modulus and the $\tan \delta$ curves were compared in Figure 5. A delay in T_g was observed on the $\tan \delta$ curves. Mostly, the glass transition obtained from the storage modulus curves has been considered to be used for the structural design of composite structural components. Additionally, the relationship between glass transition, preserved temperatures, damping properties, and frequencies was assessed from the three peak curves. The peaks of the curves show a right shift to higher values with increasing frequencies and preserved temperatures. This might occur due to reducing the crosslinking of the polymer molecules under the swelling of moisture for extended periods. It needs more heat to increase the mobility of the polymer network to turn viscous. In particular, -80°C /GCG hybrid laminates provided the highest storage modulus, damping properties, and a longer period to attain their glass transition temperatures. Based on this experimental data, the hybrid laminates that are preserved at lower temperatures for longer periods offer advantages in terms of obtaining longer lifespans and better damping properties. This could happen because it takes longer for the polymer molecules to reach the glass transition temperature.

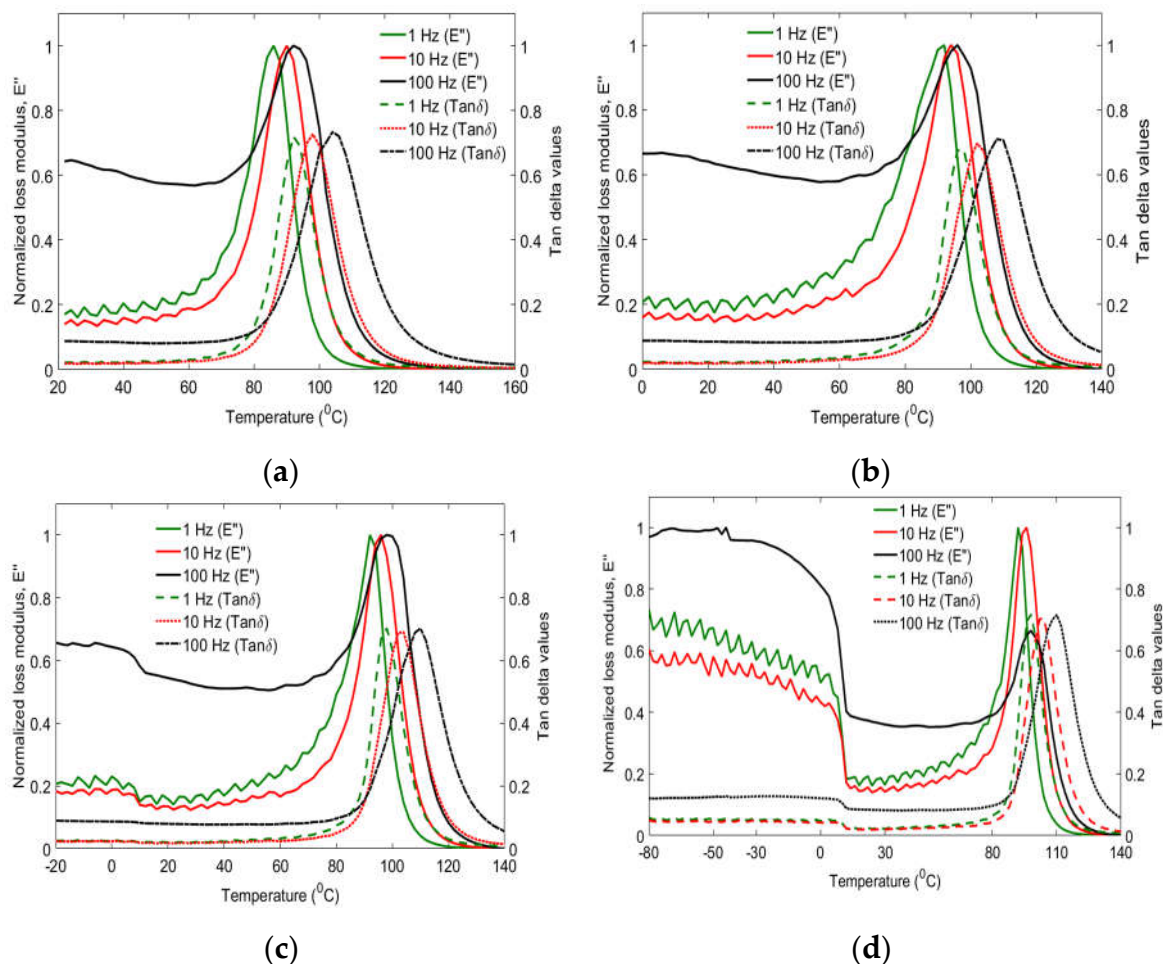


Figure 5. Loss modulus and damping properties of control GCG (a), 0°C /GCG (b), -20°C /GCG (c), and -80°C /GCG (d) laminates at various temperatures and frequencies.

The glass transition temperature of the FRP composites follows a typical Arrhenius law with the loading frequency [47]. The values of activation energy for all groups of the hybrid laminates were identified based on the Arrhenius relationship. This is represented by:

$$f = A \exp\left(-\left(\frac{E_a}{RT_g}\right)\right) \text{ or } \ln(f) = \ln(A) - \left(\frac{E_a}{R}\right) \times \left(\frac{1}{T_g}\right) \quad (2)$$

where f is the frequency, A is a constant, E_a is the activation energy, R is the universal gas constant and the T_g value is in Kelvin obtained from storage modulus, loss modulus, and $\tan \delta$ curves.

As shown in Figure 6, the targeted logarithmic frequencies and the reciprocal of the T_g values of all groups of hybrid laminates have a linear relationship. The activation energy of each hybrid laminate was obtained using the slope of $(-E_a/R)$ by the linearized curves of $\ln(f)$ versus $\left(\frac{1}{T_g}\right)$ and their values are summarized in Table 4. The linearly fitted curves were compared with the curves obtained from storage modulus, loss modulus, and $\tan \delta$ as a function of the targeted frequencies. All groups of the hybrid laminates showed a close correlation and their values were between 0.9812 and 1.

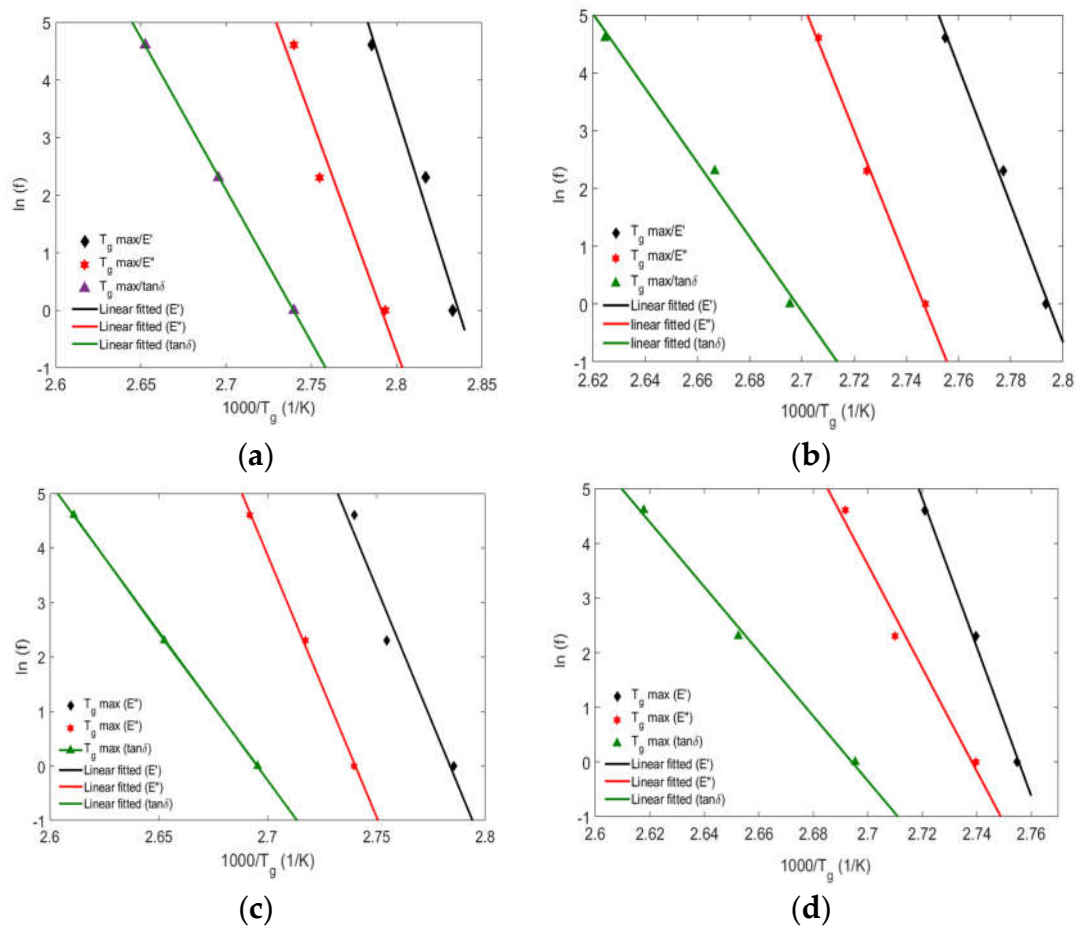


Figure 6. The logarithmic frequencies versus the reciprocal of glass transition temperatures of the GCG laminates.

Table 4. The values of activation energy (E_a) of the GCG groups of laminates obtained at the glass transition regions of the storage modulus, loss modulus, and $\tan \delta$ curves.

Activation energy (kJ/mol) Group of hybrid laminates	T_{gmax} (storage modulus)	T_{gmax} (loss modulus)	T_{gmax} ($\tan \delta$)
Control GCG	781.03	672.05	439.00
0°C/GCG	981.15	933.28	534.95
-20°C/GCG	805.02	797.49	453.33
-80°C/GCG	1130.87	783.79	491.47

4. Models of Temperature-Dependent Storage Modulus

FRP composite materials have gained widespread use in the aerospace, automotive, marine, and wind turbine blade manufacturing industries by providing lightweight, durable, and corrosion-resistant solutions for various structural components. At elevated temperatures, FRP materials have reduced mechanical properties due to the softening of the polymer matrix and degradation of the reinforcing fibers. Conversely, at low temperatures, FRP composites may become more strong, brittle, and prone to fracture. These temperature-dependent mechanical properties of FRP materials can be determined using experimental methods. It is a costly and time-consuming process to find the appropriate material to be used under different environmental conditions. A number of researchers developed analytical analyses methods to predict the mechanical properties of FRP composites as a function of temperature. For example, an empirical model was developed by Gibson et al. [45] to find the storage modulus of FRP materials as a function of temperature. The parameters under the glass transition regions were used to estimate the empirical model and were described by:

$$E(T) = \frac{E_u + E_r}{2} - \frac{E_u - E_r}{2} \tanh[k(T - T')] \quad (3)$$

where $E(T)$ is the value of storage modulus at a specified temperature T , E_u is the value of the storage modulus at room temperature, E_r is the value of storage modulus at the rubbery state, and k and T' are variables determined by fitting data using a regression analysis. The value of T' is recommended when the storage modulus of the material falls rapidly.

Most polymeric materials have four states, such as glassy (g), leathery (l), rubbery (r), and decomposition (d) states, and three transitions: glass transition, leathery to rubbery transition, and rubbery to decomposition transition. Preserving composite materials at lower temperatures for extended periods has an impact on obtaining the gamma (γ) and the beta (β) transitions in the glassy state [47]. In this case, beta (β) transition is observed in the $-20^\circ\text{C}/\text{GCG}$ and $-80^\circ\text{C}/\text{GCG}$ hybrid laminates.

Let us consider the unit volume of the initial hybrid composite laminates at specific temperatures. The volume of the laminates at different states can be determined as follows:

$$V_\beta = (1 - \beta) \quad (4)$$

$$V_g = \beta \cdot (1 - \alpha_g) \quad (5)$$

$$V_l = \beta \cdot \alpha_g \cdot (1 - \alpha_r) \quad (6)$$

$$V_r = \beta \cdot \alpha_g \cdot \alpha_r \cdot (1 - \alpha_d) \quad (7)$$

$$V_d = \beta \cdot \alpha_g \cdot \alpha_r \cdot \alpha_d \quad (8)$$

where V is the volume of the laminates in different states.

Assuming that E_β , E_g , E_l , E_r and E_d are the storage moduli in the specified states, the values of the storage modulus at a different state E_m is determined by:

$$E_m = E_\beta \cdot (1 - \beta) + E_g \cdot \beta \cdot (1 - \alpha_g) + E_l \cdot \beta \cdot \alpha_g \cdot (1 - \alpha_r) + E_r \cdot \beta \cdot \alpha_g \cdot \alpha_r \cdot (1 - \alpha_d) + E_d \cdot \beta \cdot \alpha_g \cdot \alpha_r \cdot \alpha_d \quad (9)$$

Considering that the storage moduli of the laminates at the leathery and rubbery states is nearly the same and neglecting the β transitions, Eq. (9) can be reduced to:

$$E_m = E_g \cdot (1 - \alpha_g) + E_r \cdot \alpha_g \cdot (1 - \alpha_d) \quad (10)$$

Comparison of the Storage Modulus Results with Analytical Models

The experimental results obtained on GCG hybrid composite laminates as a function of temperature and frequency are compared with the empirical models specified in Eqs. (3) and (10). Close correlations with minimum errors were observed.

Figure 7 shows the storage modulus of the control GCG composite laminate compared with the empirical models specified in Eqs. (3) and (10). The minimum errors observed using Eq. (3) are 0.50% and 0.43% at frequencies of 1 Hz and 100 Hz, respectively. Meanwhile, the errors are reduced below 0.02% in the case of Eq. (10). Moreover, the empirical models are further compared with the storage modulus of the hybrid laminates preserved at different temperatures for extended periods. Figure 8 shows the comparison between the storage modulus of 0°C/GCG laminates with the specified empirical models at frequencies of 1 Hz and 100 Hz. The minimum errors obtained using Eq. (3) are 0.39% and 0.60% at frequencies of 1 Hz and 100 Hz, respectively. However, the errors are reduced below 0.02% in the case of Eq. (10). In all cases, both empirical models have a very close correlation with the storage modulus.

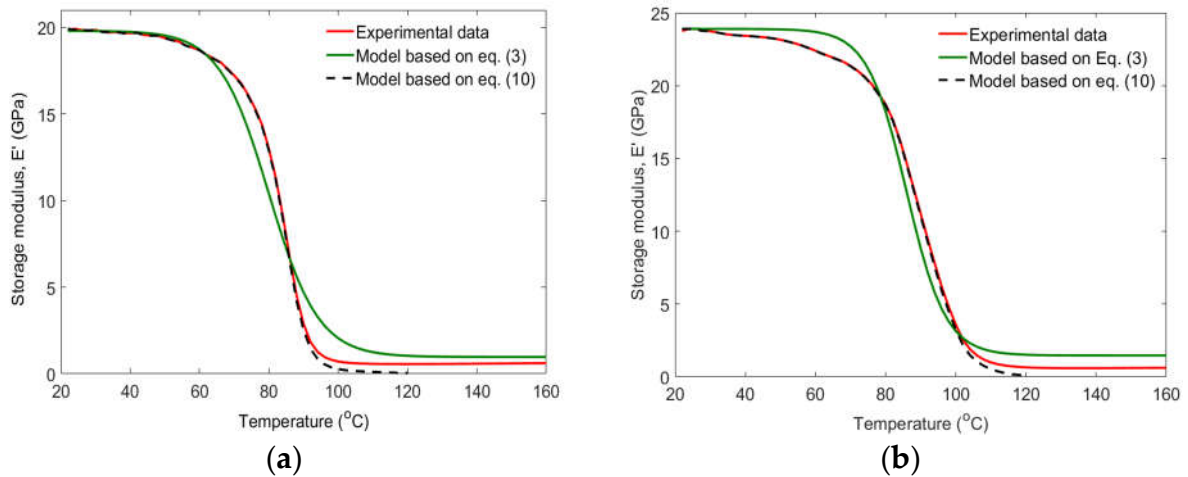


Figure 7. Comparisons between the storage modulus data and empirical models for control GCG laminates at 1 Hz (a) and 100 Hz (b).

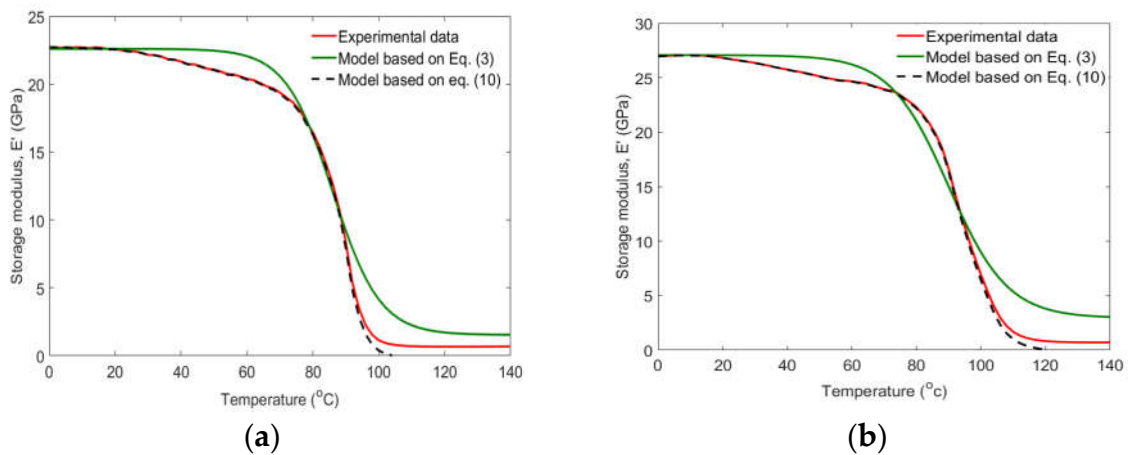


Figure 8. Comparisons between the storage modulus data and empirical models for 0°C/GCG laminates at 1 Hz (a) and 100 Hz (b).

Furthermore, a comparison is made between the storage modulus of -20°C/GCG laminates and the empirical models as shown in Figure 9. The minimum errors obtained using Eq. (3) are 0.39% and 0.37% at frequencies of 1 Hz and 100 Hz, respectively. However, close correlations are observed and the minimum errors are reduced below 0.03% with the empirical model specified in Eq. (10). The curves generated using the theoretical modulus exhibit a proper fit with the storage modulus results.

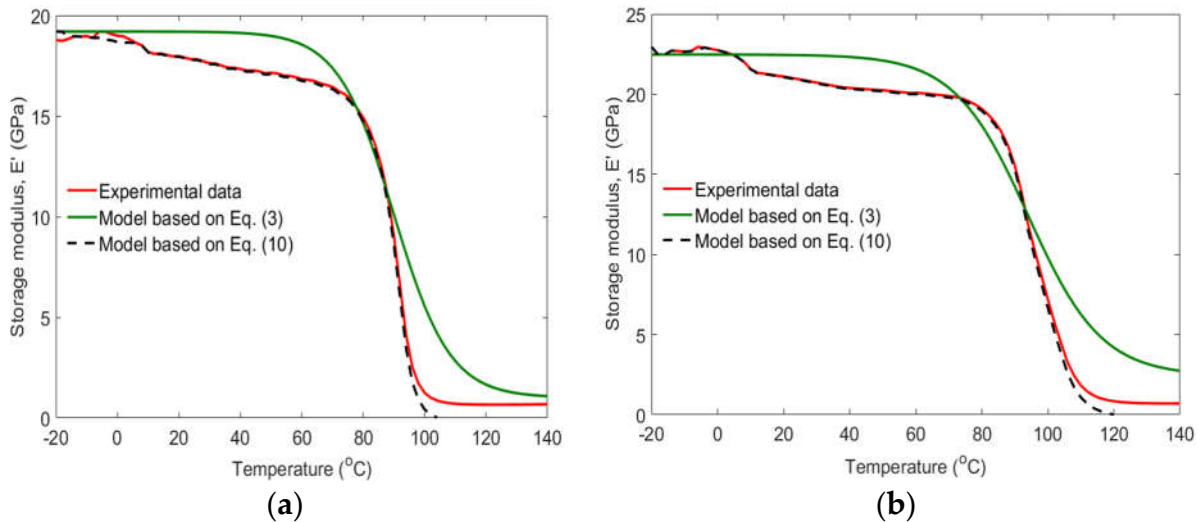


Figure 9. Comparisons between the storage modulus data and empirical models for -20°C /GCG laminates at 1 Hz (a) and 100 Hz (b).

Figure 10 shows the comparison between the storage modulus of the -80°C/GCG composite laminates and the specified empirical models. The empirical model proposed by Gibson et al. [45] exhibits significant deviations from the storage modulus curves with the minimum errors approaching 5%. Notably, it lacks close correlations with the experimental data at a lower preservation temperature for extended periods. The theoretical model, with the formulation based on the principles of Arrhenius's law, exhibits properly fitted curves that closely align with the storage modulus results. Arrhenius's law is often employed to describe the temperature dependence of various material properties, in particular, in the context of kinetics. In general, the utilization of Arrhenius's law in developing the theoretical model enhances our understanding of the temperature-dependent properties of the FRP composite materials and reinforces the predictive power of the model in capturing its mechanical behavior across different temperatures and frequencies.

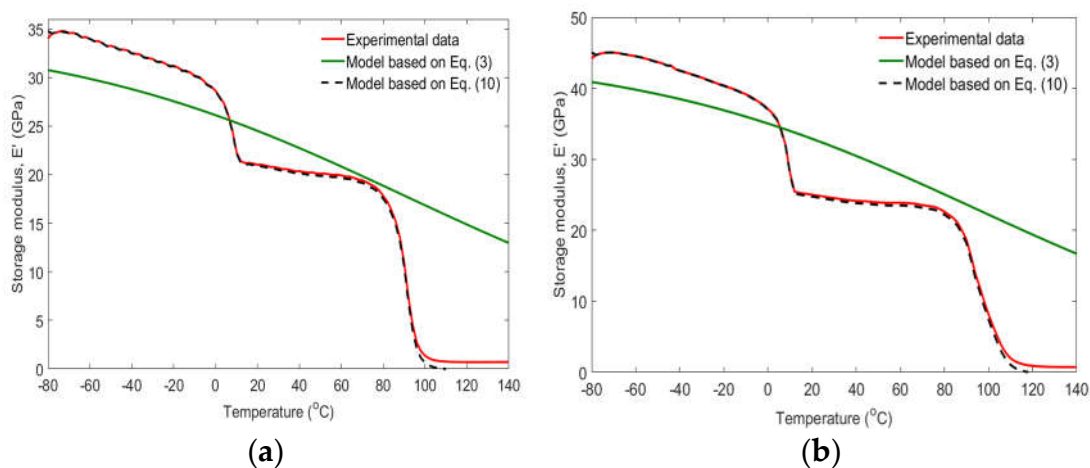


Figure 10. Comparisons between the storage modulus data and empirical models for -80°C/GCG laminates at 1 Hz (a) and 100 Hz (b).

5. Conclusions

The effect of long-term perseveration of GCG laminates under different environmental conditions is examined using a tensile testing machine and a DMA tool. Tensile, compressive, and stiffness parameters, such as the storage modulus, loss modulus, and damping properties are characterized. Additionally, the storage modulus of the hybrid laminates is validated with different empirical models. The following observations and conclusions are obtained:

1. The highest and the lowest compressive strength properties were obtained when the GCG laminates were tested at temperatures of -80°C and 100°C , respectively. The highest compressive values were obtained due to the prolonged swallow of moisture that increases the crosslinking of the polymer network and has the highest brittle property. The lowest value was obtained due to an increase in the mobility of the polymer material under increasing testing temperatures.
2. The values of the tensile strength and tensile modulus of GCG composite laminates exhibited minor differences when testing the samples after being preserved over extended periods. Both properties were reduced at the test temperature of 50°C . This indicates the initial onset of the mobility of polymeric matrix material that reduces the transfer capacity of the loads to the fibres before reaching the glass transition temperature.
3. The stiffness parameters such as storage modulus, loss modulus, and damping properties of the GCG laminates were decreased as the testing temperature approached the glass transition. The highest stiffness parameter was observed in the case of $-80^{\circ}\text{C}/\text{GCG}$ laminates. This might occur due to the existence of beta transition on the glassy regions.
4. The storage modulus of GCG laminates is compared with empirical models. The model developed using the Arrhenius law was found to be accurate in predicting laminates tested under different temperatures and frequencies. The model developed using Gibson et al. [45] needs further research to predicate the storage modulus of laminates persevered at lower temperatures.

Author Contributions: G.T. reviewed papers, designed the study, prepared fibres and polymers, and then manufactured the laminates, conducted testing, compared the experimental results with the empirical models, prepared the article; G.B. supported preparing the material, edited the article, and S.A. supported preparing the material and reviewed the article.

Funding: Please add: This research received no external funding.

Institutional Review Board Statement: Not applicable.

Data Availability Statement: Data presented in this study are available in the article.

Acknowledgments: We gratefully acknowledge the facilities provided by the University of KwaZulu-Natal (UKZN), South Africa.

Conflicts of Interest: The authors declare no conflict of interest.

References

1. Vieira, P.S.C.; de Souza, F.S.; Cardoso, D.C.T.; Vieira, J.D.; Silva, F.d.A. Influence of moderate/high temperatures on the residual flexural behavior of pultruded GFRP. *Compos. Part B: Eng.* **2020**, *200*, <https://doi.org/10.1016/j.compositesb.2020.108335>.
2. Guermazi, N.; Ben Tarjem, A.; Ksouri, I.; Ayedi, H.F. On the durability of FRP composites for aircraft structures in hygrothermal conditioning. *Compos. Part B: Eng.* **2016**, *85*, 294–304, <https://doi.org/10.1016/j.compositesb.2015.09.035>.
3. Bazli, M.; Jafari, A.; Ashrafi, H.; Zhao, X.-L.; Bai, Y.; Raman, R.S. Effects of UV radiation, moisture and elevated temperature on mechanical properties of GFRP pultruded profiles. *Constr. Build. Mater.* **2020**, *231*, <https://doi.org/10.1016/j.conbuildmat.2019.117137>.
4. Rajak, D.K.; Wagh, P.H.; Linul, E. Manufacturing Technologies of Carbon/Glass Fiber-Reinforced Polymer Composites and Their Properties: A Review. *Polymers* **2021**, *13*, 3721, <https://doi.org/10.3390/polym13213721>.
5. Pérez-Pacheco, E.; Cauich-Cupul, J.I.; Valadez-González, A.; Herrera-Franco, P.J. Effect of moisture absorption on the mechanical behavior of carbon fiber/epoxy matrix composites. *J. Mater. Sci.* **2012**, *48*, 1873–1882, <https://doi.org/10.1007/s10853-012-6947-4>.

6. Wang, T.; Song, B.; Qiao, K.; Ding, C.; Wang, L. Influence of the hybrid ratio and stacking sequence on mechanical and damping properties of hybrid composites. *Polym. Compos.* **2018**, *40*, 2368–2380, <https://doi.org/10.1002/pc.25096>.
7. Cavalcanti, D.; Vidal, M.; Jr, H. L. O.; Ornaghi, F. G.; Monticeli, F. M.; Hila, M. O. Effect of different stacking sequences on hybrid carbon/glass / epoxy composites laminate: Thermal, dynamic mechanical and long-term behavior. *J. Compos. Mater.* **2020**, *54*(6), 731–743.
8. Correia, J. R.; Gomes, M. M.; Pires, J. M.; Branco, F. A. Mechanical behavior of Pultruded glass fibre reinforced polymer composites at elevated temperature: Experiments and model assessment. *Compos. Struct.* **2013**, *98*, 303–313.
9. Sujon, A.S.; Habib, M.A.; Abedin, M.Z. Experimental investigation of the mechanical and water absorption properties on fiber stacking sequence and orientation of jute/carbon epoxy hybrid composites. *J. Mater. Res. Technol.* **2020**, *9*, 10970–10981, <https://doi.org/10.1016/j.jmrt.2020.07.079>.
10. Alessi, S.; Pitarresi, G.; Spadaro, G. Effect of hydrothermal ageing on the thermal and delamination fracture behaviour of CFRP composites. *Compos. Part B: Eng.* **2014**, *67*, 145–153, <https://doi.org/10.1016/j.compositesb.2014.06.006>.
11. Liu, T.; Liu, X.; Feng, P. A comprehensive review on mechanical properties of pultruded FRP composites subjected to long-term environmental effects. *Compos. Part B: Eng.* **2020**, *191*, 107958, <https://doi.org/10.1016/j.compositesb.2020.107958>.
12. Frigione, M.; Lettieri, M. Durability Issues and Challenges for Material Advancements in FRP Employed in the Construction Industry. *Polymers* **2018**, *10*, 247, <https://doi.org/10.3390/polym10030247>.
13. Bazli, M.; Abolfazli, M. Mechanical Properties of Fibre Reinforced Polymers under Elevated Temperatures: An Overview. *Polymers* **2020**, *12*, 2600, <https://doi.org/10.3390/polym12112600>.
14. Mlyniec, A.; Korta, J.; Kudelski, R.; Uhl, T. The influence of the laminate thickness, stacking sequence and thermal aging on the static and dynamic behavior of carbon/epoxy composites. *Compos. Struct.* **2014**, *118*, 208–216, <https://doi.org/10.1016/j.compstruct.2014.07.047>.
15. Aklilu, G.; Adali, S.; Bright, G. Tensile behaviour of hybrid and non-hybrid polymer composite specimens at elevated temperatures. *Eng. Sci. Technol. Int. J.* **2019**, *23*, 732–743, <https://doi.org/10.1016/j.jestch.2019.10.003>.
16. Cao, S.; Wu, Z.; Wang, X. Tensile Properties of CFRP and Hybrid FRP Composites at Elevated Temperatures. *J. Compos. Mater.* **2009**, *43*, 315–330, <https://doi.org/10.1177/0021998308099224>.
17. Jia, Z.; Li, T.; Chiang, F.-P.; Wang, L. An experimental investigation of the temperature effect on the mechanics of carbon fiber reinforced polymer composites. *Compos. Sci. Technol.* **2018**, *154*, 53–63, <https://doi.org/10.1016/j.compscitech.2017.11.015>.
18. Tefera, G.; Adali, S.; Bright, G. Mechanical behaviour of carbon fibre reinforced polymer composite material at different temperatures: Experimental and model assessment. *Polym. Polym. Compos.* **2022**, *30*, <https://doi.org/10.1177/09673911221125072>.
19. Zhou, F.; Zhang, J.; Song, S.; Yang, D.; Wang, C. Effect of Temperature on Material Properties of Carbon Fiber Reinforced Polymer (CFRP) Tendons: Experiments and Model Assessment. *Materials* **2019**, *12*, 1025, doi:10.3390/ma12071025.
20. Bazli, M.; Ashrafi, H.; Oskouei, A.V. Effect of harsh environments on mechanical properties of GFRP pultruded profiles. *Compos. Part B: Eng.* **2016**, *99*, 203–215, <https://doi.org/10.1016/j.compositesb.2016.06.019>.
21. Wang, K.; Young, B.; Smith, S.T. Mechanical properties of pultruded carbon fibre-reinforced polymer (CFRP) plates at elevated temperatures. *Eng. Struct.* **2011**, *33*, 2154–2161, <https://doi.org/10.1016/j.engstruct.2011.03.006>.
22. Jarrah, M.; Najafabadi, E.P.; Khaneghahi, M.H.; Oskouei, A.V. The effect of elevated temperatures on the tensile performance of GFRP and CFRP sheets. *Constr. Build. Mater.* **2018**, *190*, 38–52, <https://doi.org/10.1016/j.conbuildmat.2018.09.086>.
23. Jafari, A.; Bazli, M.; Ashrafi, H.; Oskouei, A.V.; Azhari, S.; Zhao, X.-L.; Gholipour, H. Effect of fibers configuration and thickness on tensile behavior of GFRP laminates subjected to elevated temperatures. *Constr. Build. Mater.* **2019**, *202*, 189–207, <https://doi.org/10.1016/j.conbuildmat.2019.01.003>.
24. Hawileh, R. A.; Obeidah, A. A.; Abdalla, J. A.; Tamimi, A. A. Temperature effect on the mechanical properties of carbon, glass and carbon-glass FRP laminates. *Constr. Build. Mater.* **2015**, *75*, 342–348.
25. Zafar, A.; Bertocco, F.; Schjødt-Thomsen, J.; Rauhe, J. Investigation of the long term effects of moisture on carbon fibre and epoxy matrix composites. *Compos. Sci. Technol.* **2012**, *72*, 656–666, <https://doi.org/10.1016/j.compscitech.2012.01.010>.
26. Aniskevich, K.; Aniskevich, A.; Arnautov, A.; Jansons, J. Mechanical properties of pultruded glass fiber-reinforced plastic after moistening. *Compos. Struct.* **2012**, *94*, 2914–2919, <https://doi.org/10.1016/j.compstruct.2012.04.030>.

27. Bazli, M.; Ashrafi, H.; Jafari, A.; Zhao, X.-L.; Raman, R.S.; Bai, Y. Effect of Fibers Configuration and Thickness on Tensile Behavior of GFRP Laminates Exposed to Harsh Environment. *Polymers* **2019**, *11*, 1401, <https://doi.org/10.3390/polym11091401>.
28. Reyes, L.Q.; Swan, S.R.; Gan, H.; Seraji, S.M.; Zhang, J.; Varley, R.J. The role of β relaxations in determining the compressive properties of an epoxy amine network modified with POSS and mono-functional epoxy resins. *Polym. Test.* **2020**, *93*, 106873, <https://doi.org/10.1016/j.polymertesting.2020.106873>.
29. Tefera, G.; Adali, S.; Bright, G. Mechanical Behavior of GFRP Laminates Exposed to Thermal and Moist Environmental Conditions: Experimental and Model Assessment. *Polymers* **2022**, *14*, 1523, <https://doi.org/10.3390/polym14081523>.
30. Spagnuolo, S.; Meda, A.; Rinaldi, Z.; Nanni, A. Residual behaviour of glass FRP bars subjected to high temperatures. *Compos. Struct.* **2018**, *203*, 886–893, <https://doi.org/10.1016/j.compstruct.2018.07.077>.
31. Robert, M.; Benmokrane, B. Behavior of GFRP Reinforcing Bars Subjected to Extreme Temperatures. *J. Compos. Constr.* **2010**, *14*, 353–360.
32. Lundgren, J.-E.; Gudmundson, P. Moisture absorption in glass-fibre/epoxy laminates with transverse matrix cracks. *Compos. Sci. Technol.* **1999**, *59*, 1983–1991, [https://doi.org/10.1016/s0266-3538\(99\)00055-x](https://doi.org/10.1016/s0266-3538(99)00055-x).
33. Ellyin, F.; Rohrbacher, C. Effect of aqueous environment and temperature on glass-fibre epoxy resin composites. *J. Reinf. Plast. Compos.* **2000**, *17*, 1405–1423.
34. Behera, A.; Vishwakarma, A.; Thawre, M.; Ballal, A. Effect of hygrothermal aging on static behavior of quasi-isotropic CFRP composite laminate. *Compos. Commun.* **2019**, *17*, 51–55, <https://doi.org/10.1016/j.coco.2019.11.009>.
35. Karvanis, K.; Rusnáková, S.; Žaludek, M.; Čapka, A. Preparation and Dynamic Mechanical Analysis of Glass or carbon Fiber/Polymer Composites. *IOP Conf. Series: Mater. Sci. Eng.* **2018**, *362*, 012005, <https://doi.org/10.1088/1757-899x/362/1/012005>.
36. Trauth, A.; Kirchenbauer, K.; Weidenmann, K. Dynamic-mechanical-thermal analysis of hybrid continuous-discontinuous sheet molding compounds. *Compos. Part C: Open Access* **2021**, *5*, 100148, <https://doi.org/10.1016/j.jcomc.2021.100148>.
37. Alvarez, V.; Valdez, M.; Vázquez, A. Dynamic mechanical properties and interphase fiber/matrix evaluation of unidirectional glass fiber/epoxy composites. *Polym. Test.* **2003**, *22*, 611–615, [https://doi.org/10.1016/s0142-9418\(02\)00164-2](https://doi.org/10.1016/s0142-9418(02)00164-2).
38. Tsai, Y.; Bosze, E.; Barjasteh, E.; Nutt, S. Influence of hygrothermal environment on thermal and mechanical properties of carbon fiber/fiberglass hybrid composites. *Compos. Sci. Technol.* **2008**, *69*, 432–437, <https://doi.org/10.1016/j.compscitech.2008.11.012>.
39. Bai, Y.; Keller, T. Time Dependence of Material Properties of FRP Composites in Fire. *J. Compos. Mater.* **2009**, *43*, 2469–2484, <https://doi.org/10.1177/0021998309344641>.
40. Mouritz, A.; Feih, S.; Kandare, E.; Mathys, Z.; Gibson, A.; Jardin, P.D.; Case, S.; Lattimer, B. Review of fire structural modelling of polymer composites. *Compos. Part A: Appl. Sci. Manuf.* **2009**, *40*, 1800–1814, <https://doi.org/10.1016/j.compositesa.2009.09.001>.
41. Mahieux, C.A.; Reifsnider, K.L. Property modeling across transition temperatures in polymers: application to thermoplastic systems. *J. Mater. Sci.* **2002**, *37*, 911–920, <https://doi.org/10.1023/a:1014383427444>.
42. Bai, Y.; Keller, T. Modeling of post-fire stiffness of E-glass fiber-reinforced polyester composites. *Compos. Part A: Appl. Sci. Manuf.* **2007**, *38*, 2142–2153, <https://doi.org/10.1016/j.compositesa.2007.06.010>.
43. Aklilu, G.; Adali, S.; Bright, G. Long-term effects of low and high temperatures on the mechanical performance of hybrid FRP composite laminates: Experimental and model assessment. *Compos. Part C: Open Access* **2023**, *11*, <https://doi.org/10.1016/j.jcomc.2023.100352>.
44. Bai, Y.; Keller, T. Modeling of Strength Degradation for Fiber-reinforced Polymer Composites in Fire. *J. Compos. Mater.* **2009**, *43*, 2371–2385, <https://doi.org/10.1177/0021998309344642>.
45. Gibson, A.G.; Wu, Y.-S.; Evans, J.T.; Mouritz, A.P. Laminate Theory Analysis of Composites under Load in Fire. *J. Compos. Mater.* **2005**, *40*, 639–658, <https://doi.org/10.1177/0021998305055543>.
46. Bai, Y.; Keller, T.; Vallée, T. Modeling of stiffness of FRP composites under elevated and high temperatures. *Compos. Sci. Technol.* **2008**, *68*, 3099–3106, <https://doi.org/10.1016/j.compscitech.2008.07.005>.
47. Feng, J.; Guo, Z. Temperature-frequency-dependent mechanical properties model of epoxy resin and its composites. *Compos. Part B: Eng.* **2016**, *85*, 161–169, <https://doi.org/10.1016/j.compositesb.2015.09.040>.
48. Aklilu, G.; Adali, S.; Bright, G. Experimental Characterization of Hybrid and Non-Hybrid Polymer Composites at Elevated Temperatures. *Int. J. Eng. Res. Afr.* **2018**, *36*, 37–52, <https://doi.org/10.4028/www.scientific.net/JERA.36.37>.
49. ASTM D 695 standard test method for compressive properties of plastic materials SRM 1R-94, ASTM International: West Conshohocken, PA, USA, 2002.
50. ASTM 3039/D 3039M standard test method for tensile properties of polymer matrix composite materials, ASTM International: West Conshohocken, PA: USA, 2002.
51. Menard, K. Dynamic mechanical analysis: a practical introduction; Boca Raton, FL: CRC Press, 2008.

52. ASTM D 3171 Standard Test Methods for Constituent Content of Composite Materials, ASTM International: West Conshohocken, PA, USA, 2000.

Disclaimer/Publisher's Note: The statements, opinions and data contained in all publications are solely those of the individual author(s) and contributor(s) and not of MDPI and/or the editor(s). MDPI and/or the editor(s) disclaim responsibility for any injury to people or property resulting from any ideas, methods, instructions or products referred to in the content.